



OpenAIR@RGU

The Open Access Institutional Repository at Robert Gordon University

<http://openair.rgu.ac.uk>

This is an author produced version of a paper published in

IET Control Theory and Applications (ISSN 1751-8644, eISSN 1751-8652)

This version may not include final proof corrections and does not include published layout or pagination.

Citation Details

Citation for the version of the work held in 'OpenAIR@RGU':

LIU, Y., 2015. Suppressing stick-slip oscillations in underactuated multibody drill-strings with parametric uncertainties using sliding-mode control. Available from *OpenAIR@RGU*. [online]. Available from: <http://openair.rgu.ac.uk>

Citation for the publisher's version:

LIU, Y., 2015. Suppressing stick-slip oscillations in underactuated multibody drill-strings with parametric uncertainties using sliding-mode control. *IET Control Theory and Applications*, 9 (1), pp. 91-102.

Copyright

Items in 'OpenAIR@RGU', Robert Gordon University Open Access Institutional Repository, are protected by copyright and intellectual property law. If you believe that any material held in 'OpenAIR@RGU' infringes copyright, please contact openair-help@rgu.ac.uk with details. The item will be removed from the repository while the claim is investigated.

This paper is a postprint of a paper submitted to and accepted for publication in IET Control Theory and Applications and is subject to Institution of Engineering and Technology Copyright. The copy of record is available at IET Digital Library.

Suppressing Stick-Slip Oscillations in Underactuated Multibody Drill-Strings with Parametric Uncertainties using Sliding-Mode Control

Yang Liu^a

^a*School of Engineering, Robert Gordon University, Garthdee Road, Aberdeen, Scotland, UK, AB10 7GJ
(e-mail: y.liu8@rgu.ac.uk)*

Abstract

Stabilization of multibody drill-strings which exhibit stick-slip oscillations is studied in this paper from the point of view of underactuated system. The model has one control torque input acting on the rotary table from the land surface and multi-degree-of-freedom downhole parts to be controlled. Three motion regimes of the model including bit sticking, stick-slip oscillation, and rotating at a constant speed are identified and their equilibria are analyzed accordingly. The control objective of the system is to avoid the undesired bit sticking and stick-slip oscillation while tracking a desired angular velocity. Three sliding-mode controllers are studied for the drill-string with estimated physical parameters. The stabilities of the proposed controllers are proved by using the Lyapunov direct method ensuring that any trajectory of the system can reach and stays thereafter on the pre-designed sliding surface where the desired equilibrium is asymptotically stable. Extensive simulation results are given to demonstrate the effectiveness of the proposed controllers and their robustness to parametric uncertainties.

Keywords: drill-string, underactuated system, stick-slip, sliding-mode control, parametric uncertainty

1. Introduction

For conventional rotary drilling, the entire drill-string is driven by a rotary table from the land surface actuated by an electrical motor with a mechanical transmission box (see Fig. 1). The drill-string consists of a series of hollow drill pipes followed by the

bottom-hole assembly (BHA) which comprises several relatively thicker drill collars, with a number of intermediate stabilizers, terminating with a drill bit. The drill collars are relatively heavier and stiffer than drill pipes for preventing the drill-string from underbalancing which also provide necessary thrust force for drilling progression. The drill-string may run several kilometres deep, while its diameter typically does not exceed 0.3 metres [1]. This extreme slenderness of the drill-string makes it prone to exhibit complex dynamical phenomena which include undesired oscillations. Stick-slip, bit bouncing, and whirl motions are three main harmful oscillations that must be suppressed during drilling operation. Indeed, stick-slip oscillations exist in the 50% of drilling time [2], and the whipping and high speed rotations of the bit in the slip phase may cause both severe bit bouncing phenomena and whirl motion at the BHA [3].

This paper studies the stick-slip oscillations of drill-string using a lumped-parameter model, and proposes to use sliding-mode control method to suppress the oscillation when the physical parameters of the drill-string in extreme rough circumstance are unknown. Due to the speed-dependent nature of the contact force at the bit-rock interface, downhole conditions, e.g. significant drag or sudden change of drilled formation may cause the drill bit to stall in the formation while the rotary table above the land surface continues to rotate. When the trapped torsional energy at the motionless drill bit reaches a limit, the drill bit suddenly becomes loose, rotating and whipping at a very high speed. The consequence of the stick-slip oscillation is that the rotary speed of the drill bit varies from zero up to several times the rotary speed of the rotary table which reduces penetration rate and increases costly failures. An example of stick-slip oscillations of a drill-string is shown in Fig. 2 using time histories of angular velocities of the rotary table (marked by black dash line) and the drill bit (shown by red solid line) driving by a constant control torque. As can be seen from the figure, the bit is stuck at the beginning due to friction. Once the driving torque on bit is greater than the torque of friction, the bit suddenly becomes loose and rotates drastically. After a short while, the rotary speed of the bit reduces and the bit is stuck again. The stick-slip motion can generate a torsional wave that travels up the drill-

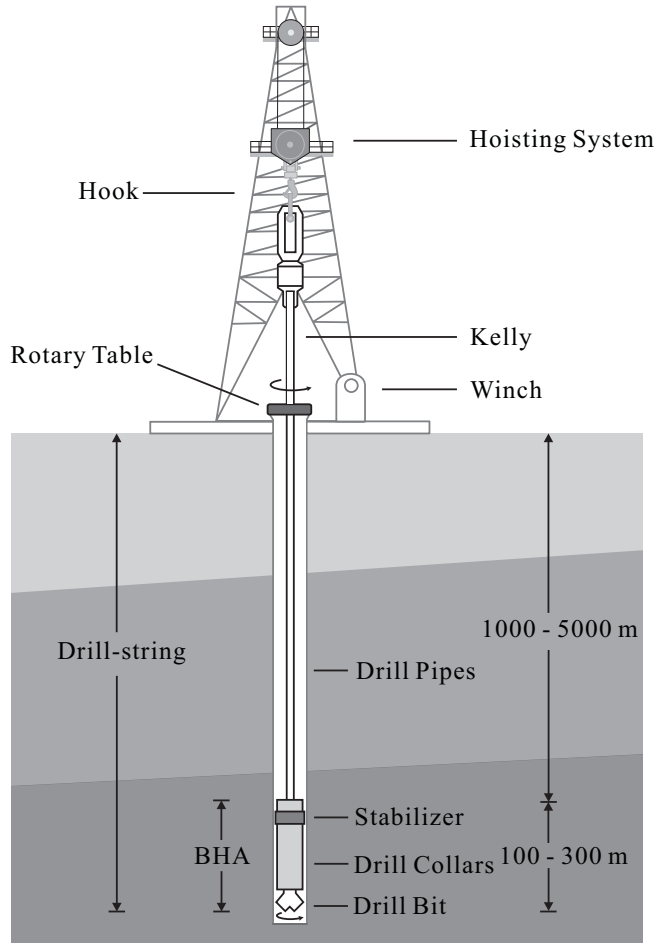


Figure 1: Schematic view of an oilwell drilling rig.

string to the land surface which oscillates the rotary table accordingly. This behaviour is harmful not only for damaging the top drive system but also for causing uncontrollable bit motions in both axial and lateral directions. Therefore the control objective for the drill-string is to make the drill bit suppress the stick-slip oscillation whilst tracking a desired constant angular velocity with the presence of unknown parameters and downhole frictions.

The schematics of the drill-string is presented in Fig. 3(a), and its simplified lumped-parameter model is shown in Fig. 3(b). The literature using the lumped-parameter model for control purpose is vast, e.g. [4, 5, 6, 7, 8]. Navarro-López and Cortés [4] used a generic lumped-parameter model to analyze self-excited stick-slip oscillations at

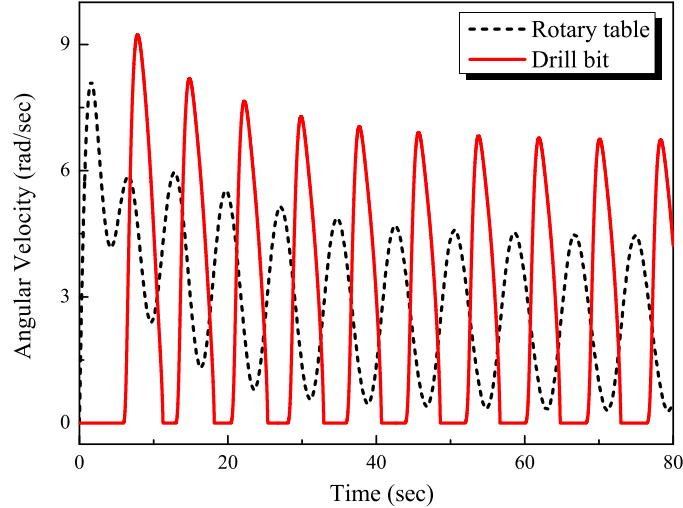


Figure 2: The stick-slip oscillations of a drill-string: time histories of angular velocities of the rotary table (marked by black dash line) and the drill bit (shown by red solid line) driving by a constant control torque.

the drill bit by identifying the ranges of key drilling parameters for which non-desired torsional oscillations can be avoided. In [5], Navarro-López and Licéaga-Castro proposed a dynamical sliding-mode controller to avoid different bit sticking problems appearing in the model. Canudas-de-Wit *et al.* [6] proposed to use the weight on bit (WOB) as a control variable for extinguishing stick-slip oscillations. In [7], a control approach based on the modelling error compensation technique was studied in order to provide robustness against uncertain parameters and frictions. Karkoub *et al.* [8] addressed the problem of suppressing stick-slip oscillations using the μ -synthesis control technique which allowed for modelling errors in terms of uncertain WOB. However the dynamic model of the drill-string has to be linearized around an operating point for applying the μ -synthesis technique. So the performance of the controller cannot be guaranteed if more underactuated degrees of freedom are considered. As manipulating the WOB in downhole environment could be problematic, this paper proposes to use sliding-mode control strategy to suppress the stick-slip oscillation by applying torque control to the rotary table only. The difference between the existing sliding-mode controllers, e.g. [5, 9, 10] and the proposed one is that the latter has tolerance for parameter uncertainties and is robust to the variation of WOB as measuring all these physical parameters precisely in

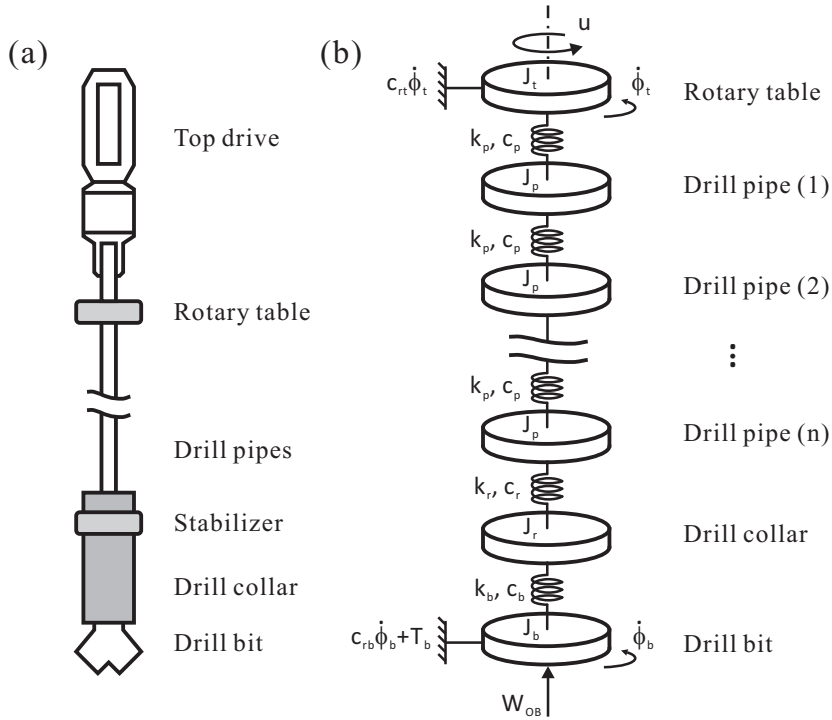


Figure 3: Schematics of (a) a drill-string and (b) a simplified drill-string model

borehole is unrealistic.

The drill-string is an underactuated system [11] as it has one control torque input actuating on the rotary table from the ground and multi-degree-of-freedom downhole parts comprising the drill pipes, the drill collars and the drill bit to be controlled. For traditional underactuated systems, friction is always omitted or simplified despite it plays a significant role in some engineering applications, e.g. [12, 13]. For underactuated drill-strings, a comprehensive friction model is vital for depicting bit-rock contact in borehole but meanwhile will induce undesired motion regimes, i.e. bit sticking and stick-slip oscillation, and the existence of these regimes depends on the WOB and the control torque input. Compared to traditional underactuated systems, the drill-string has different equilibria for these regimes and the proposed control method should allow its trajectory track a desired equilibrium within a desired regime while avoiding the other undesired ones. In addition, the variation of the WOB during drilling affects the existence of the undesired regimes which can result in severe drilling failure. So a proper control design which is not

only able to track a desired equilibrium but also has robustness to the variation of system parameter in a dynamic varying environment is crucial.

In recent years, sliding-mode control of underactuated systems has focused on some specific systems, such as surface vessel [14, 15], wheeled inverted pendulum [16], mobile robot [17], and crane system [18, 19], as well as for a class of underactuated systems, e.g. [20, 21, 22, 23, 24]. In [20], a sliding-mode controller was proposed for a class of underactuated multibody systems, and the stability of the sliding surface based on the equilibrium manifold was discussed. In [21], a sliding-mode control approach which can globally stabilize all degrees of freedom including the degrees which were indirectly actuated through the nonlinear coupling was studied for a class of underactuated systems. In [22], a hybrid sliding-mode controller was studied for a class of underactuated systems with dry friction. The method allows to control the actuated and unactuated links separately with known friction level at the unactuated link. In [23], Sankaranarayanan and Mahindrakar proposed a switching surface design for a class of underactuated systems, and studied a switched algorithm to make the system state reach the surface in finite time using conventional higher order sliding-mode controller. López-Martínez *et al.* [24] proposed a nonlinear sliding surface design through a fictitious output which provided the minimum-phase property of a class of non-minimum phase underactuated systems. In general, the basic idea of these methods is to alter the dynamics of the system by applying a discontinuous control input that makes the system state ‘slide’ along a predefined surface, and then the system state tracks the desired trajectory by being restricted to the surface. However the switching state of the system along the surface leads to chattering which cannot be implemented by practical systems. Thus two continuous switching functions are proposed in this paper to replace the discontinuous function in traditional sliding-mode controller conducting a chattering-free control. Although continuous switching functions have been used in many sliding-mode controllers, very few of them have been applied to underactuated systems and no theoretical proof can be found.

The rest of this paper is organized as follows. In Section 2, the lumped-parameter

model of an underactuated multibody drill-string is introduced. The friction model representing rock-bit contact is studied, and the occurrence of the stick-slip phenomena is explained. Three motion regimes of the model are identified and their corresponding equilibria are analyzed. In Section 3, three sliding-mode controllers are studied and their stabilities are proved by using the Lyapunov direct method. In Section 4, simulation results are given to demonstrate the effectiveness of the proposed controllers and their robustness to parametric uncertainties. Finally, conclusions are drawn in Section 5.

2. Drill-string model and its equilibria

2.1. The lumped-parameter model

The lumped-parameter model of a drill-string shown in Fig. 3(b) can be written as

$$J\ddot{\Phi} + C\dot{\Phi} + K\Phi + T = U, \quad (1)$$

where $\Phi = [\phi_t, \phi_1, \phi_2, \dots, \phi_n, \phi_r, \phi_b]^T \in \mathfrak{R}^{(n+3) \times 1}$ is the angular position of the lumped mass, $J = \text{diag}(J_t, \underbrace{J_p, J_p, \dots, J_p}_n, J_r, J_b) \in \mathfrak{R}^{(n+3) \times (n+3)}$ is the inertia matrix, $C \in \mathfrak{R}^{(n+3) \times (n+3)}$ is the torsional damping matrix given by

$$C = \begin{bmatrix} c_p + c_{rt} & -c_p & 0 & 0 & \dots & 0 & 0 & 0 & 0 \\ -c_p & 2c_p & -c_p & 0 & \dots & 0 & 0 & 0 & 0 \\ 0 & -c_p & 2c_p & -c_p & \dots & 0 & 0 & 0 & 0 \\ \dots & \dots \\ 0 & 0 & 0 & 0 & \dots & -c_p & c_p + c_r & -c_r & 0 \\ 0 & 0 & 0 & 0 & \dots & 0 & -c_r & c_r + c_b & -c_b \\ 0 & 0 & 0 & 0 & \dots & 0 & 0 & -c_b & c_b + c_{rb} \end{bmatrix},$$

$K \in \mathfrak{R}^{(n+3) \times (n+3)}$ is the torsional stiffness matrix given by

$$K = \begin{bmatrix} k_p & -k_p & 0 & 0 & \dots & 0 & 0 & 0 & 0 & 0 \\ -k_p & 2k_p & -k_p & 0 & \dots & 0 & 0 & 0 & 0 & 0 \\ 0 & -k_p & 2k_p & -k_p & \dots & 0 & 0 & 0 & 0 & 0 \\ \dots & \dots \\ 0 & 0 & 0 & 0 & \dots & -k_p & k_p + k_r & -k_r & 0 & 0 \\ 0 & 0 & 0 & 0 & \dots & 0 & -k_r & k_r + k_b & -k_b & 0 \\ 0 & 0 & 0 & 0 & \dots & 0 & 0 & -k_b & k_b & 0 \end{bmatrix},$$

$T = [0, 0, \dots, T_b]^T \in \mathfrak{R}^{(n+3) \times 1}$ is the torque of friction, and $U = [u, 0, \dots, 0]^T \in \mathfrak{R}^{(n+3) \times 1}$ is the control torque input.

Eq. (1) simplifies the torsional model of a conventional drill-string which includes a rotary table with the inertia J_t , a series of drill pipes with the inertia J_p for each pipe, a drill collar with the inertia J_r , and a drill bit with the inertia J_b . Torsional stiffness k_p and damping c_p are considered between the connection of each lumped mass from the rotary table to the n^{th} drill pipe. The torsional stiffness and damping between the n^{th} drill pipe and the drill collar are k_r and c_r , respectively. The torsional stiffness and damping between the drill collar and the drill bit are k_b and c_b , respectively. The control input of the drill-string is the drive torque u from the electrical motor at the land surface, and a viscous damping torque $c_{rt}\dot{\phi}_t$ is considered on the rotary table corresponding to the lubrication of the mechanical elements of the top drive system, where c_{rt} is the viscous damping coefficient. A viscous damping torque $c_{rb}\dot{\phi}_b$ is considered on the drill bit representing the influence of the drilling mud on the bit. T_b is the torque of friction when the drill bit contacts with the rock given by

$$T_b = \begin{cases} \tau_r & \text{if } |\dot{\phi}_b| < \zeta \text{ and } |\tau_r| \leq \tau_s, \\ \tau_s \text{sgn}(\tau_r) & \text{if } |\dot{\phi}_b| < \zeta \text{ and } |\tau_r| > \tau_s, \\ \mu_b R_b W_{ob} \text{sgn}(\dot{\phi}_b) & \text{if } |\dot{\phi}_b| \geq \zeta. \end{cases} \quad (2)$$

The friction model contains the following three phases.

- Sticking phase ($|\dot{\phi}_b| < \zeta$ and $|\tau_r| \leq \tau_s$): the bit velocity is less than a small positive constant ζ , and the reaction torque τ_r is less or equals to the static friction torque τ_s , where

$$\tau_r = c_b(\dot{\phi}_r - \dot{\phi}_b) + k_b(\phi_r - \phi_b) - c_{rb}\dot{\phi}_b,$$

$\tau_s = \mu_{sb}R_bW_{ob}$, μ_{sb} is the static friction coefficient, W_{ob} is the WOB, and R_b is the bit radius. In the sticking phase, the bit is stalled in borehole.

- Stick-to-slip transition phase ($|\dot{\phi}_b| < \zeta$ and $|\tau_r| > \tau_s$): the bit velocity is still less than the constant ζ , but the reaction torque τ_r is greater than the static friction torque τ_s . So the drill bit just begins to rotate from stationary.
- Slip phase ($|\dot{\phi}_b| \geq \zeta$): the calculation of frictional torque includes the effects of the bit radius R_b , the WOB W_{ob} , and the bit dry friction coefficient $\mu_b = \mu_{cb} + (\mu_{sb} - \mu_{cb})e^{-\gamma_b|\dot{\phi}_b|/v_f}$, where μ_{cb} is the Coulomb friction coefficient, $0 < \gamma_b < 1$ is a constant defining the velocity decrease rate of T_b , and v_f is a velocity constant.

2.2. Analysis of equilibria

Let Γ_b be a switching manifold

$$\Gamma_b := \{\Phi \in \mathfrak{R}^{(n+3) \times 1} : \dot{\phi}_b = 0\} \quad (3)$$

and $\tilde{\Gamma}_b$ be an attractive region

$$\tilde{\Gamma}_b := \{\Phi \in \Gamma_b : |c_b\dot{\phi}_r + k_b(\phi_r - \phi_b)| < \mu_{sb}R_bW_{ob}\} \quad (4)$$

which is a subset of Γ_b . Due to the presence of friction at the bit-rock interface, three motion regimes for the drill-string driven by a constant torque can be identified:

- The bit is permanently stuck in borehole, i.e. for $\forall t > t_{sb}$, $\Phi \in \tilde{\Gamma}_b$, where t_{sb} is the time that system trajectory reaches $\tilde{\Gamma}_b$ and stays in the region thereafter;

- The bit is in stick-slip oscillations, i.e. the trajectory of the drill-string enters and leaves $\tilde{\Gamma}_b$ repeatedly;
- The bit moves at a positive constant speed.

Let us define a new state of the system as

$$x = [\dot{\phi}_t, \phi_t - \phi_1, \dot{\phi}_1, \phi_1 - \phi_2, \dots, \dot{\phi}_n, \phi_n - \phi_r, \dot{\phi}_r, \phi_r - \phi_b, \dot{\phi}_b]^T.$$

The regime of bit sticking has an asymptotically stable equilibrium given by

$$x_s = [0, \frac{u}{k_p}, 0, \frac{u}{k_p}, \dots, 0, \frac{u}{k_p}, 0, \frac{u}{k_r}, 0, \frac{u}{k_b}, 0]^T,$$

and the standard equilibrium when the bit moves at a positive constant speed is

$$x_c = [\Omega_c, \frac{h}{k_p}, \Omega_c, \frac{h}{k_p}, \dots, \Omega_c, \frac{h}{k_p}, \Omega_c, \frac{h}{k_r}, \Omega_c, \frac{h}{k_b}, \Omega_c]^T,$$

where Ω_c is a constant speed depending on W_{ob} and u , $h = \frac{c_{rt}T_b(\Omega_c, W_{ob}) + c_{rb}u}{(c_{rt} + c_{rb})}$, and $(c_{rt} + c_{rb})\Omega_c + T_b(\Omega_c, W_{ob}) = u$ which can be obtained from Eq. (1).

The control objective for the drill-string is to avoid the regimes of bit sticking and stick-slip oscillation whilst tracking a desired constant angular velocity Ω_d using the control input u only with estimated physical parameters. It is worth noting that the standard equilibrium is locally asymptotically stable depending on W_{ob} , u , and Ω_c , and the loss of stability is due to the presence of Hopf bifurcations [5]. The desired angular velocity Ω_d has to be chosen away from the bifurcation velocity Ω^* (i.e. $\Omega_d > \Omega^*$). Therefore in the following control design, we assume that (1) W_{ob} is small enough and (2) u is sufficiently large so that the desired velocity Ω_d exists.

Fig. 4 presents a series of bifurcation diagrams showing the evolution of the motion regimes for the drill-string with $n = 4$ under variation of WOB. The simulations were run for 300 seconds and the data for the first 200 seconds were omitted to ensure the

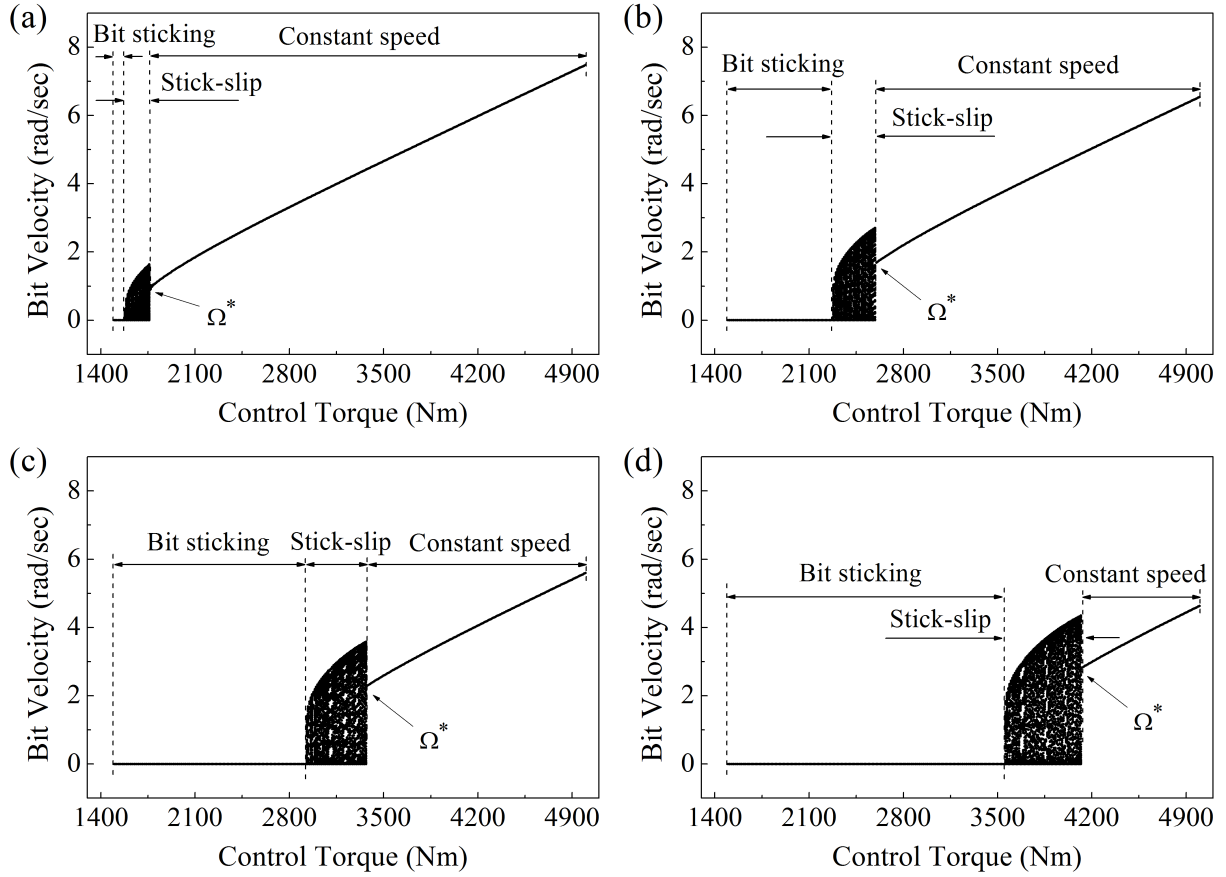


Figure 4: Bifurcation diagrams for the drill-string with $n = 4$ for varying the control torque, u with (a) $W_{ob} = 20$ kN; (b) $W_{ob} = 30$ kN; (c) $W_{ob} = 40$ kN; and (d) $W_{ob} = 50$ kN.

steady state response, whereas the next 100 seconds of the bit velocity were plotted in the bifurcation diagrams for each value of the constant control torque. As can be seen from Fig. 4(a), the bit is stuck in borehole when the constant control torque is small, and the regime of stick-slip oscillation is observed once the control torque is increased. When the control torque is sufficiently large, the bit rotates at a constant positive speed. From Fig. 4(b)-(d), it can be seen that the existing ranges of the undesired regimes are enlarged due to the increase of WOB. This observation confirms that the equilibria of the drill-string are dependent on WOB and the desired angular velocity Ω_d has to be chosen as $\Omega_d > \Omega^*$ which ensures that the desired equilibrium is locally asymptotically stable.

3. Sliding-mode control

For the purpose of control design, the new state of the system is defined as

$$\begin{aligned} x &= [\dot{\phi}_t, \phi_t - \phi_1, \dot{\phi}_1, \phi_1 - \phi_2, \dots, \dot{\phi}_n, \phi_n - \phi_r, \dot{\phi}_r, \phi_r - \phi_b, \dot{\phi}_b]^T \\ &= [x_1, x_2, x_3, x_4, \dots, x_{2n+1}, x_{2n+2}, x_{2n+3}, x_{2n+4}, x_{2n+5}]^T, \end{aligned}$$

and the drill-string model in Eq. (1) can be rewritten as

$$\begin{aligned} \dot{x}_1 &= J_t^{-1}[u - (c_p + c_{rt})x_1 + c_p x_3 - k_p x_2], \\ \dot{x}_2 &= x_1 - x_3, \\ \dot{x}_3 &= J_1^{-1}(c_p x_1 - 2c_p x_3 + c_p x_5 + k_p x_2 - k_p x_4), \\ \dot{x}_4 &= x_3 - x_5, \\ &\dots \\ \dot{x}_{2n+1} &= J_n^{-1}[c_p x_{2n-1} - (c_p + c_r) x_{2n+1} + c_r x_{2n+3} + k_p x_{2n} - k_r x_{2n+2}], \\ \dot{x}_{2n+2} &= x_{2n+1} - x_{2n+3}, \\ \dot{x}_{2n+3} &= J_r^{-1}[c_r x_{2n+1} - (c_r + c_b) x_{2n+3} + c_b x_{2n+5} + k_r x_{2n+2} - k_b x_{2n+4}], \\ \dot{x}_{2n+4} &= x_{2n+3} - x_{2n+5}, \\ \dot{x}_{2n+5} &= J_b^{-1}[c_b x_{2n+3} - (c_b + c_{rb}) x_{2n+5} + k_b x_{2n+4} - T_b]. \end{aligned} \tag{5}$$

Define the sliding surface as

$$s = (x_1 - \Omega_d) + \lambda \int_0^t (x_1 - \Omega_d) d\tau + \lambda \int_0^t (x_1 - x_{2n+5}) d\tau, \tag{6}$$

where λ is a positive constant selected by designer, and the time derivative of the sliding surface can be written as

$$\dot{s} = \dot{x}_1 + \lambda(x_1 - \Omega_d) + \lambda(x_1 - x_{2n+5}). \tag{7}$$

Substituting \dot{x}_1 in Eq. (7) using the new state vector gives

$$\dot{s} = J_t^{-1}[u - (c_p + c_{rt})x_1 + c_p x_3 - k_p x_2] + \lambda(x_1 - \Omega_d) + \lambda(x_1 - x_{2n+5}). \quad (8)$$

The ideal controller without any parametric uncertainties can be derived from the solution of $\dot{s} = 0$ as

$$u_{ideal} = (c_p + c_{rt})x_1 - c_p x_3 + k_p x_2 - J_t \lambda(x_1 - \Omega_d) - J_t \lambda(x_1 - x_{2n+5}). \quad (9)$$

Now define the sliding-mode controller as

$$u = u_{eq} + u_{sw}, \quad (10)$$

where u_{eq} is the equivalent control, and u_{sw} is the switching control of the sliding-mode controller. The equivalent control is obtained from Eq. (9) as

$$u_{eq} = (\hat{c}_p + \hat{c}_{rt})x_1 - \hat{c}_p x_3 + \hat{k}_p x_2 - \hat{J}_t \lambda(x_1 - \Omega_d) - \hat{J}_t \lambda(x_1 - x_{2n+5}), \quad (11)$$

where “ $\hat{}$ ” indicates the estimated model parameter, and the switching control is given by

$$u_{sw}^I = -\sigma \text{sgn}(s), \quad (12)$$

where σ is the reaching control gain associated with the upper bounds of uncertainties, and the discontinuous sign function can be written as

$$\text{sgn}(s) = \begin{cases} 1 & \text{if } s > 0, \\ 0 & \text{if } s = 0, \\ -1 & \text{if } s < 0. \end{cases}$$

A general structure of the control system is shown in Fig 5. It is worth noting that the control design in this paper assumes that all the required states of the system, $x_1, x_2, x_3,$

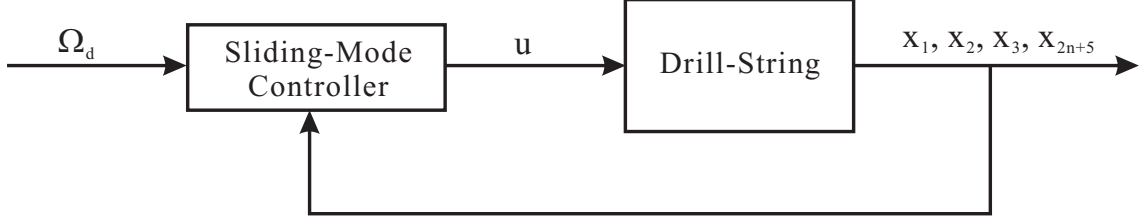


Figure 5: General structure of the proposed sliding-mode controller

and x_{2n+5} , are directly measurable. In real practice, such a measurement is difficult due to delays and noise in downhole and an observer-based controller is always preferable, e.g. [25, 26]. However as this is outside of the scope of this paper, such results will be reported in a separated publication in due course.

Theorem 1. *If the upper bounds of the estimated model parameters are known as*

$$|\hat{c}_p - c_p| \leq M_{cp}, \quad |\hat{c}_{rt} - c_{rt}| \leq M_{crt}, \quad |\hat{k}_p - k_p| \leq M_{kp}, \quad |\hat{J}_t - J_t| \leq M_{jt},$$

and the switching control gain is chosen as

$$\sigma = M_{cp}|x_1 - x_3| + M_{crt}|x_1| + M_{kp}|x_2| + M_{jt}\lambda|x_1 - \Omega_d| + M_{jt}\lambda|x_1 - x_{2n+5}| + \eta, \quad (13)$$

where η is a positive constant, by applying the sliding-mode control (10)-(12), any trajectory of the system can reach and stays thereafter on the manifold $s = 0$ in finite time.

Proof. Let choose the following Lyapunov function

$$V = \frac{1}{2} J_t s^2, \quad (14)$$

and the time derivative of V can be written as

$$\dot{V} = J_t s \dot{s}. \quad (15)$$

Substituting \dot{s} in Eq. (15) using Eq. (8) gives

$$\dot{V} = s[u - (c_p + c_{rt})x_1 + c_p x_3 - k_p x_2 + J_t \lambda (x_1 - \Omega_d) + J_t \lambda (x_1 - x_{2n+5})], \quad (16)$$

Applying the sliding-mode control (10), Eq. (16) becomes

$$\begin{aligned}\dot{V} &= s[(\hat{c}_p - c_p)(x_1 - x_3) + (\hat{c}_{rt} - c_{rt})x_1 + (\hat{k}_p - k_p)x_2 \\ &\quad + (J_t - \hat{J}_t)\lambda(x_1 - \Omega_d) + (J_t - \hat{J}_t)\lambda(x_1 - x_{2n+5}) - \sigma \operatorname{sgn}(s)].\end{aligned}\quad (17)$$

Since the switching control gain is chosen as Eq. (13), the time derivative of V can be rewritten as

$$\begin{aligned}\dot{V} &= s[(\hat{c}_p - c_p)(x_1 - x_3) + (\hat{c}_{rt} - c_{rt})x_1 + (\hat{k}_p - k_p)x_2 \\ &\quad + (J_t - \hat{J}_t)\lambda(x_1 - \Omega_d) + (J_t - \hat{J}_t)\lambda(x_1 - x_{2n+5}) \\ &\quad - M_{cp}|x_1 - x_3|\operatorname{sgn}(s) - M_{crt}|x_1|\operatorname{sgn}(s) - M_{kp}|x_2|\operatorname{sgn}(s) \\ &\quad - M_{jt}\lambda|x_1 - \Omega_d|\operatorname{sgn}(s) - M_{jt}\lambda|x_1 - x_{2n+5}|\operatorname{sgn}(s) - \eta \operatorname{sgn}(s)] \\ &\leq -\eta|s| \leq 0.\end{aligned}\quad (18)$$

So by applying the sliding-mode controller (10)-(12) with the reaching control gain (13), the trajectory of the drill-string can reach and stays thereafter on the manifold $s = 0$ in finite time. ■

Proposition 1. *Once the trajectory of the drill-string stays on the manifold $s = 0$, the state of the system asymptotically converges to the desired equilibrium*

$$\begin{aligned}\bar{x} &= [\bar{x}_1, \bar{x}_2, \bar{x}_3, \bar{x}_4, \dots, \bar{x}_{2n+1}, \bar{x}_{2n+2}, \bar{x}_{2n+3}, \bar{x}_{2n+4}, \bar{x}_{2n+5}]^T \\ &= [\Omega_d, \frac{\bar{h}}{k_p}, \Omega_d, \frac{\bar{h}}{k_p}, \dots, \Omega_d, \frac{\bar{h}}{k_p}, \Omega_d, \frac{\bar{h}}{k_r}, \Omega_d, \frac{\bar{h}}{k_b}, \Omega_d]^T,\end{aligned}$$

where $\bar{h} = c_{rb}\Omega_d + T_b(\Omega_d)$ is a positive constant.

Proof. Define a new Lyapunov function

$$\begin{aligned}\bar{V} &= \frac{1}{2}[J_t(x_1 - \bar{x}_1)^2 + k_p(x_2 - \bar{x}_2)^2 + J_1(x_3 - \bar{x}_3)^2 + k_p(x_4 - \bar{x}_4)^2 \\ &\quad + \dots + J_n(x_{2n+1} - \bar{x}_{2n+1})^2 + k_r(x_{2n+2} - \bar{x}_{2n+2})^2 \\ &\quad + J_r(x_{2n+3} - \bar{x}_{2n+3})^2 + k_b(x_{2n+4} - \bar{x}_{2n+4})^2 + J_b(x_{2n+5} - \bar{x}_{2n+5})^2],\end{aligned}\quad (19)$$

and its time derivative is written as

$$\begin{aligned}
\dot{\hat{V}} &= J_t(x_1 - \bar{x}_1)\dot{x}_1 + k_p(x_2 - \bar{x}_2)\dot{x}_2 + J_1(x_3 - \bar{x}_3)\dot{x}_3 + k_p(x_4 - \bar{x}_4)\dot{x}_4 \\
&+ \dots + J_n(x_{2n+1} - \bar{x}_{2n+1})\dot{x}_{2n+1} + k_r(x_{2n+2} - \bar{x}_{2n+2})\dot{x}_{2n+2} \\
&+ J_r(x_{2n+3} - \bar{x}_{2n+3})\dot{x}_{2n+3} + k_b(x_{2n+4} - \bar{x}_{2n+4})\dot{x}_{2n+4} \\
&+ J_b(x_{2n+5} - \bar{x}_{2n+5})\dot{x}_{2n+5}.
\end{aligned} \tag{20}$$

Since the trajectory of the drill-string is on the sliding surface $s = 0$, the equivalent control on the surface can be obtained from the solution of $\dot{s} = 0$ as

$$u_{eq}^* = (c_p + c_{rt})x_1 - c_p x_3 + k_p x_2 - J_t \lambda (x_1 - \Omega_d) - J_t \lambda (x_1 - x_{2n+5}), \tag{21}$$

which equals to the equivalent control in Eq. (11). Applying Eq. (5) and (21), Eq. (20) becomes

$$\begin{aligned}
\dot{\hat{V}} &= -c_{rt}(x_1 - \Omega_d)^2 - c_p(x_1 - x_3)^2 - c_p(x_3 - x_5)^2 \dots \\
&- c_r(x_{2n+1} - x_{2n+3})^2 - c_b(x_{2n+3} - x_{2n+5})^2 - c_{rb}(x_{2n+5} - \Omega_d)^2.
\end{aligned} \tag{22}$$

Therefore $\dot{\hat{V}} \leq 0$, and $\dot{\hat{V}} = 0$ only for $x = \bar{x}$. ■

Remark 1. *As when the system trajectory approaches to the manifold $s = 0$, it is switched around the manifold by the discontinuous sign function in Eq. (12) which will induce high-frequency chattering to the control torque input and thereby the drill-string state. The chattering is harmful as such a high-frequency switching control could damage the top drive system on the land surface and influences drill-string stability.*

In order to overcome this issue, the following theorem is proposed.

Theorem 2. *If the modified switching control*

$$u_{sw}^{\text{II}} = -\sigma \frac{s}{|s| + \delta} - \kappa s, \tag{23}$$

is applied, where δ and κ are small positive constants selected by designer, the tracking errors of the drill-string are asymptotically bounded.

Proof. See Appendix. ■

Remark 2. The parameter δ can be selected as small as possible such that $\delta \rightarrow 0$ leading to $\|s\| \rightarrow 0$ so that $x \rightarrow \bar{x}$. However if the parameter δ is too small, the continuous function $\frac{s}{|s+\delta|}$ becomes discontinuous so that the chattering will be introduced to the system again.

Since the second switching control (23) is only asymptotically bounded not asymptotically convergent, the following new switching control is proposed.

Theorem 3. If the switching control is chosen as

$$u_{sw}^{\text{III}} = -\frac{M_{cp}|x_1-x_3|s}{|s+\delta_1 \exp(-\delta_2 \int |\dot{x}_2| dt)} - \frac{M_{crt}|x_1|s}{|s+\delta_1 \exp(-\delta_2 \int |x_1| dt)} - \frac{M_{kp}|x_2|s}{|s+\delta_1 \exp(-\delta_2 \int |x_2| dt)} - \frac{M_{jt}\lambda|x_1-\Omega_d|s}{|s+\delta_1 \exp(-\delta_2 \int \lambda|x_1-\Omega_d| dt)} - \frac{M_{jt}\lambda|x_1-x_{2n+5}|s}{|s+\delta_1 \exp(-\delta_2 \int \lambda|x_1-x_{2n+5}| dt)} - \kappa s, \quad (24)$$

where δ_1 and δ_2 are small positive constants selected by designer, the trajectory of the drill-string will reach the sliding surface asymptotically, and the state of the system will asymptotically converge to the desired equilibrium \bar{x} .

Proof. In order to prove the stability of the third switching control (24), a new Lyapunov function is defined as

$$\begin{aligned} V &= \frac{1}{2} J_t s^2 + M_{cp} \frac{\delta_1}{\delta_2} \exp(-\delta_2 \int |\dot{x}_2| dt) + M_{crt} \frac{\delta_1}{\delta_2} \exp(-\delta_2 \int |x_1| dt) \\ &+ M_{kp} \frac{\delta_1}{\delta_2} \exp(-\delta_2 \int |x_2| dt) + M_{jt} \frac{\delta_1}{\delta_2} \exp(-\delta_2 \int \lambda|x_1 - \Omega_d| dt) \\ &+ M_{jt} \frac{\delta_1}{\delta_2} \exp(-\delta_2 \int \lambda|x_1 - x_{2n+5}| dt). \end{aligned} \quad (25)$$

From the strict definition of the Lyapunov function, although the new function (25) is positive definite but not a legitimate Lyapunov function since $\forall t \geq 0, V(0) \neq 0$. So the following additional state is introduced.

$$z = [z_1, z_2, z_3, z_4, z_5]^T,$$

where

$$\begin{aligned} z_1 &= \sqrt{2M_{cp} \frac{\delta_1}{\delta_2} \exp(-\delta_2 \int |\dot{x}_2| dt)} \\ z_2 &= \sqrt{2M_{crt} \frac{\delta_1}{\delta_2} \exp(-\delta_2 \int |x_1| dt)} \\ z_3 &= \sqrt{2M_{kp} \frac{\delta_1}{\delta_2} \exp(-\delta_2 \int |x_2| dt)} \\ z_4 &= \sqrt{2M_{jt} \frac{\delta_1}{\delta_2} \exp(-\delta_2 \int \lambda|x_1 - \Omega_d| dt)} \\ z_5 &= \sqrt{2M_{jt} \frac{\delta_1}{\delta_2} \exp(-\delta_2 \int \lambda|x_1 - x_{2n+5}| dt)}. \end{aligned}$$

Thus Eq. (25) becomes

$$V = \frac{1}{2} J_t s^2 + \frac{1}{2} z^T z = \frac{1}{2} J_t s^2 + \frac{1}{2} \sum_{i=1}^5 z_i^2. \quad (26)$$

As $t \rightarrow \infty$, z_i is exponentially convergent to zero leading to $V \rightarrow 0$ when $s = 0$. So Eq. (26) is a legitimate Lyapunov function with state variables $[s, z^T]^T$, and the time derivative of Eq. (26) is given by

$$\begin{aligned} \dot{V} &= J_t s \dot{s} - M_{cp} \delta_1 |\dot{x}_2| \exp(-\delta_2 \int |\dot{x}_2| dt) - M_{crt} \delta_1 |x_1| \exp(-\delta_2 \int |x_1| dt) \\ &\quad - M_{kp} \delta_1 |x_2| \exp(-\delta_2 \int |x_2| dt) - M_{jt} \delta_1 \lambda |x_1 - \Omega_d| \exp(-\delta_2 \int \lambda |x_1 - \Omega_d| dt) \\ &\quad - M_{jt} \delta_1 \lambda |x_1 - x_{2n+5}| \exp(-\delta_2 \int \lambda |x_1 - x_{2n+5}| dt). \end{aligned} \quad (27)$$

Applying the sliding-mode control (10) using the equivalent control (11) and the third switching control (24), Eq. (27) becomes

$$\begin{aligned} \dot{V} &= s[(\hat{c}_p - c_p)(x_1 - x_3) + (\hat{c}_{rt} - c_{rt})x_1 + (\hat{k}_p - k_p)x_2 + (J_t - \hat{J}_t)\lambda(x_1 - \Omega_d) \\ &\quad + (J_t - \hat{J}_t)\lambda(x_1 - x_{2n+5}) - \frac{M_{cp}|x_1 - x_3|s}{|s| + \delta_1 \exp(-\delta_2 \int |\dot{x}_2| dt)} - \frac{M_{crt}|x_1|s}{|s| + \delta_1 \exp(-\delta_2 \int |x_1| dt)} \\ &\quad - \frac{M_{kp}|x_2|s}{|s| + \delta_1 \exp(-\delta_2 \int |x_2| dt)} - \frac{M_{jt}\lambda|x_1 - \Omega_d|s}{|s| + \delta_1 \exp(-\delta_2 \int \lambda |x_1 - \Omega_d| dt)} - \frac{M_{jt}\lambda|x_1 - x_{2n+5}|s}{|s| + \delta_1 \exp(-\delta_2 \int \lambda |x_1 - x_{2n+5}| dt)} - \kappa s] \\ &\quad - M_{cp} \delta_1 |\dot{x}_2| \exp(-\delta_2 \int |\dot{x}_2| dt) - M_{crt} \delta_1 |x_1| \exp(-\delta_2 \int |x_1| dt) \\ &\quad - M_{kp} \delta_1 |x_2| \exp(-\delta_2 \int |x_2| dt) - M_{jt} \delta_1 \lambda |x_1 - \Omega_d| \exp(-\delta_2 \int \lambda |x_1 - \Omega_d| dt) \\ &\quad - M_{jt} \delta_1 \lambda |x_1 - x_{2n+5}| \exp(-\delta_2 \int \lambda |x_1 - x_{2n+5}| dt) \\ &\leq |(\hat{c}_p - c_p)(x_1 - x_3)s| + |(\hat{c}_{rt} - c_{rt})x_1 s| + |(\hat{k}_p - k_p)x_2 s| + |(J_t - \hat{J}_t)\lambda(x_1 - \Omega_d)s| \\ &\quad + |(J_t - \hat{J}_t)\lambda(x_1 - x_{2n+5})s| - \frac{M_{cp}|x_1 - x_3|s^2}{|s| + \delta_1 \exp(-\delta_2 \int |\dot{x}_2| dt)} - \frac{M_{crt}|x_1|s^2}{|s| + \delta_1 \exp(-\delta_2 \int |x_1| dt)} \\ &\quad - \frac{M_{kp}|x_2|s^2}{|s| + \delta_1 \exp(-\delta_2 \int |x_2| dt)} - \frac{M_{jt}\lambda|x_1 - \Omega_d|s^2}{|s| + \delta_1 \exp(-\delta_2 \int \lambda |x_1 - \Omega_d| dt)} - \frac{M_{jt}\lambda|x_1 - x_{2n+5}|s^2}{|s| + \delta_1 \exp(-\delta_2 \int \lambda |x_1 - x_{2n+5}| dt)} - \kappa s^2 \\ &\quad - M_{cp} \delta_1 |\dot{x}_2| \exp(-\delta_2 \int |\dot{x}_2| dt) - M_{crt} \delta_1 |x_1| \exp(-\delta_2 \int |x_1| dt) \\ &\quad - M_{kp} \delta_1 |x_2| \exp(-\delta_2 \int |x_2| dt) - M_{jt} \delta_1 \lambda |x_1 - \Omega_d| \exp(-\delta_2 \int \lambda |x_1 - \Omega_d| dt) \\ &\quad - M_{jt} \delta_1 \lambda |x_1 - x_{2n+5}| \exp(-\delta_2 \int \lambda |x_1 - x_{2n+5}| dt) \end{aligned}$$

$$\begin{aligned}
&\leq |(\hat{c}_p - c_p) \delta_1(x_1 - x_3)| \exp(-\delta_2 \int |\dot{x}_2| dt) + |(\hat{c}_{rt} - c_{rt}) \delta_1 x_1| \exp(-\delta_2 \int |x_1| dt) \\
&\quad + |(\hat{k}_p - k_p) \delta_1 x_2| \exp(-\delta_2 \int |x_2| dt) + |(J_t - \hat{J}_t) \lambda \delta_1(x_1 - \Omega_d)| \exp(-\delta_2 \int \lambda |x_1 - \Omega_d| dt) \\
&\quad + |(J_t - \hat{J}_t) \lambda \delta_1(x_1 - x_{2n+5})| \exp(-\delta_2 \int \lambda |x_1 - x_{2n+5}| dt) \\
&\quad - M_{cp} \delta_1 |\dot{x}_2| \exp(-\delta_2 \int |\dot{x}_2| dt) - M_{crt} \delta_1 |x_1| \exp(-\delta_2 \int |x_1| dt) \\
&\quad - M_{kp} \delta_1 |x_2| \exp(-\delta_2 \int |x_2| dt) - M_{jt} \delta_1 \lambda |x_1 - \Omega_d| \exp(-\delta_2 \int \lambda |x_1 - \Omega_d| dt) \\
&\quad - M_{jt} \delta_1 \lambda |x_1 - x_{2n+5}| \exp(-\delta_2 \int \lambda |x_1 - x_{2n+5}| dt) - \kappa s^2 \\
&\leq -\kappa s^2 \leq 0.
\end{aligned}$$

Therefore using the third switching control (24), any trajectory of the drill-string can reach and stays thereafter on the manifold $s = 0$ asymptotically, and according to **Proposition 1**, the state of the system asymptotically converges to the desired equilibrium \bar{x} . \blacksquare

4. Simulation results

This section presents the simulation results using the proposed sliding-mode controllers. For simplicity, a four-degree-of-freedom drill-string ($n = 1$) comprising a rotary table, a drill pipe, a drill collar, and a drill bit is considered here which can be written as

$$\begin{cases}
J_t \ddot{\phi}_t + (c_p + c_{rt}) \dot{\phi}_t - c_p \phi_1 + k_p \phi_t - k_p \phi_1 = u, \\
J_1 \ddot{\phi}_1 - c_p \dot{\phi}_t + (c_p + c_r) \dot{\phi}_1 - c_r \dot{\phi}_r - k_p \phi_t + (k_p + k_r) \phi_1 - k_r \phi_r = 0, \\
J_r \ddot{\phi}_r - c_r \dot{\phi}_1 + (c_r + c_b) \dot{\phi}_r - c_b \dot{\phi}_b - k_r \phi_1 + (k_r + k_b) \phi_r - k_b \phi_b = 0, \\
J_b \ddot{\phi}_b - c_b \dot{\phi}_r + (c_b + c_{rb}) \dot{\phi}_b - k_b \phi_r + k_b \phi_b + T_b = 0,
\end{cases} \quad (28)$$

where the model parameters are given in Table 1.

Based on Eq. (6), the sliding surface is defined as

$$s = (\dot{\phi}_t - \Omega_d) + \lambda \int_0^t (\dot{\phi}_t - \Omega_d) d\tau + \lambda \int_0^t (\dot{\phi}_t - \dot{\phi}_b) d\tau, \quad (29)$$

where $\lambda = 0.3$, and the desired angular velocity is chosen as $\Omega_d = 3$ rad/sec. Assume that the upper bounds are known and given in Table 2.

Table 1: The physical parameters of the drill-string

Parameter	Value
J_t	910 kg m ²
J_1	2800 kg m ²
J_r	750 kg m ²
J_b	450 kg m ²
c_{rt}	410 N m s/rad
c_p	150 N m s/rad
c_r	190 N m s/rad
c_b	180 N m s/rad
c_{rb}	80 N m s/rad
k_p	700 N m/rad
k_r	1080 N m/rad
k_b	910 N m/rad
μ_{sb}	0.8
μ_{cb}	0.45
W_{ob}	30 kN
R_b	0.15 m
γ_b	0.85
v_f	1
ζ	10 ⁻⁶

Table 2: The estimated physical parameters and upper bounds for the proposed sliding-mode controllers

Parameter	Value
\hat{J}_t	800 kg m ²
\hat{k}_p	630 N m/rad
\hat{c}_p	120 N m s/rad
\hat{c}_{rt}	350 N m s/rad
M_{jt}	150
M_{kp}	100
M_{cp}	40
M_{crt}	70

According to **Theorem 1**, the equivalent control is obtained as

$$u_{eq} = (\hat{c}_p + \hat{c}_{rt})\dot{\phi}_t - \hat{c}_p\dot{\phi}_1 + \hat{k}_p(\phi_t - \phi_1) - \hat{J}_t\lambda(\dot{\phi}_t - \Omega_d) - \hat{J}_t\lambda(\dot{\phi}_t - \dot{\phi}_b), \quad (30)$$

and the first switching control is given by

$$\begin{aligned} u_{sw}^I &= -(M_{cp}|\dot{\phi}_t - \dot{\phi}_1| + M_{crt}|\dot{\phi}_t| + M_{kp}|\phi_t - \phi_1| \\ &\quad + M_{jt}\lambda|\dot{\phi}_t - \Omega_d| + M_{jt}\lambda|\dot{\phi}_t - \dot{\phi}_b| + \eta) \operatorname{sgn}(s). \end{aligned} \quad (31)$$

where $\eta = 1$ is used in the simulation.

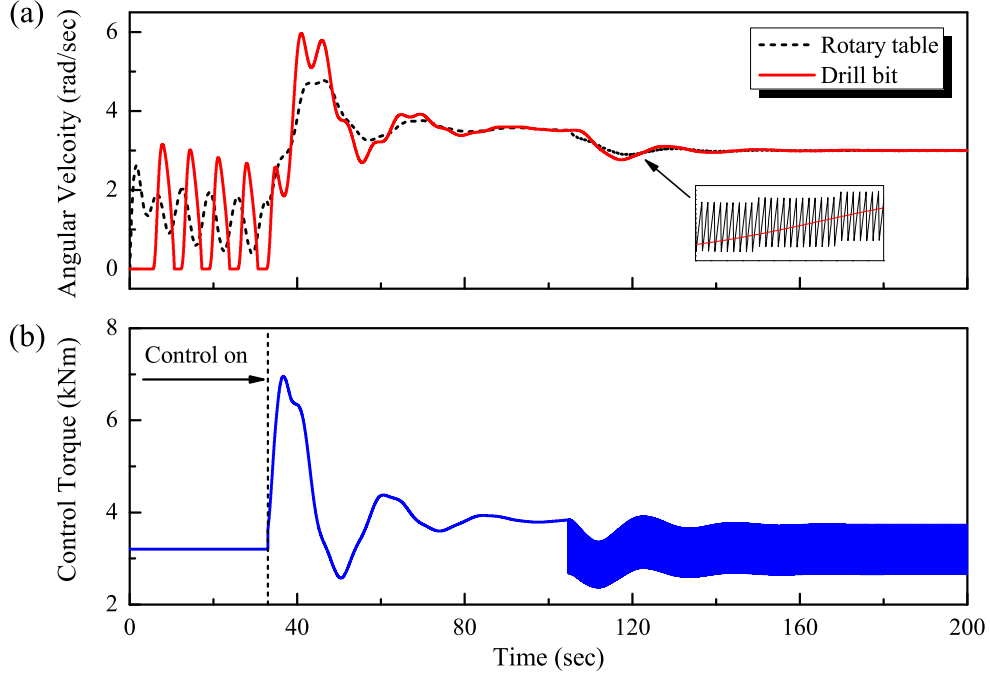


Figure 6: Time histories of (a) angular velocities of the rotary table (black dash line) and the drill bit (red solid line), and (b) the control torque (blue solid line) using the sliding-mode control (30) and (31) with $\Omega_d = 3$ rad/sec, $\lambda = 0.3$ and $\eta = 1$.

The simulation result using the sliding-mode control (30) and (31) is shown in Fig. 6. As can be seen from the figure, both the angular velocities of the rotary table and the drill bit are stabilized to the desired angular velocity at about $t = 140$ seconds. However the drill-string exhibits chattering on the rotary table and the control input when the angular velocity of the rotary table is close to the desired angular velocity.

In order to address the chattering issue, the second switching control based on **Theorem 2** is given as

$$\begin{aligned}
 u_{sw}^{\text{II}} = & -(M_{cp}|\dot{\phi}_t - \dot{\phi}_1| + M_{crt}|\dot{\phi}_t| + M_{kp}|\phi_t - \phi_1| \\
 & + M_{jt}\lambda|\dot{\phi}_t - \Omega_d| + M_{jt}\lambda|\dot{\phi}_t - \dot{\phi}_b| + \eta) \frac{s}{|s|+\delta} - \kappa s,
 \end{aligned} \tag{32}$$

where $\eta = 1$, $\delta = 0.1$ and $\kappa = 1$ are used in the simulation.

Fig. 7 shows the simulation result using the second switching control (32). It can be seen that the stick-slip oscillations were suppressed once the control was switched on

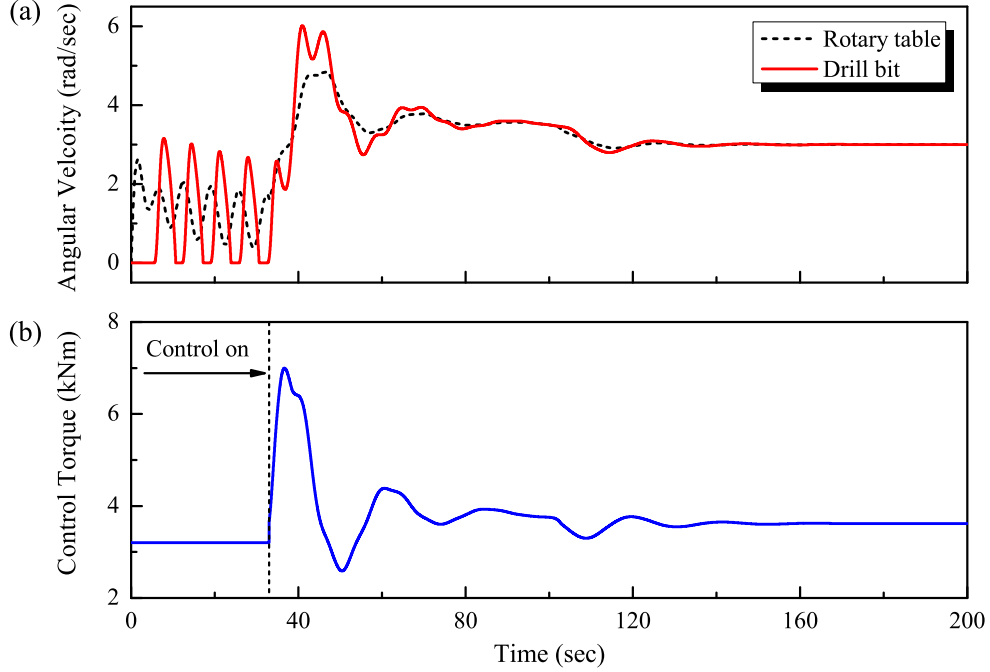


Figure 7: Time histories of (a) angular velocities of the rotary table (black dash line) and the drill bit (red solid line), and (b) the control torque (blue solid line) using the second switching control (32) with $\Omega_d = 3$ rad/sec, $\lambda = 0.3$, $\eta = 1$, $\delta = 0.1$ and $\kappa = 1$.

at $t = 33$ seconds, and the chattering of the rotary table was removed and the control input became smooth when the trajectory approached to the manifold $s = 0$. Fig. 8 presents the time histories of the control inputs using the second switching control (32) with different values of δ . As can be observed from the figure, when $\delta = 10^{-4}$, the control torque became discontinuous resulting in chattering. The comparison demonstrates that the selection of δ cannot be arbitrary small since the second switching control (32) may become discontinuous when system trajectory is close to the manifold $s = 0$. On the other hand, if δ is chosen too large, e.g. $\delta = 0.1$ as shown in Fig. 8, the trajectory of the system cannot reach an acceptable boundary of the sliding surface $s = 0$, so that a little deterioration of the tracking errors has to be compromised by choosing a proper parameter δ . In order to overcome this limitation, the third switching control based on

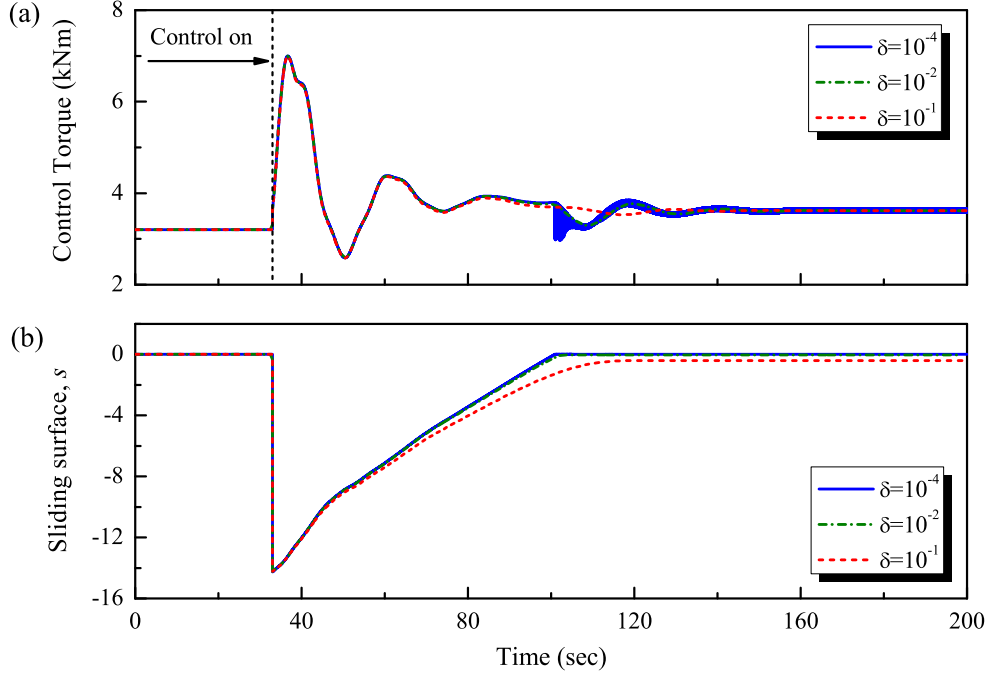


Figure 8: Time histories of (a) the control inputs using the second switching control (32) and (b) the sliding surface, s with $\Omega_d = 3$ rad/sec, $\lambda = 0.3$, $\eta = 1$, $\kappa = 1$, and different values of δ (blue solid line: $\delta = 10^{-4}$; green dash-dot line: $\delta = 0.01$; red dash line: $\delta = 0.1$).

Theorem 3 is obtained as

$$\begin{aligned}
 u_{sw}^{III} = & -\frac{M_{cp}|\dot{\phi}_t - \dot{\phi}_1|s}{|s| + \delta_1 \exp(-\delta_2 \int |\dot{\phi}_t - \dot{\phi}_1| dt)} - \frac{M_{crt}|\phi_t|s}{|s| + \delta_1 \exp(-\delta_2 \int |\phi_t| dt)} - \frac{M_{kp}|\phi_t - \phi_1|s}{|s| + \delta_1 \exp(-\delta_2 \int |\phi_t - \phi_1| dt)} \\
 & - \frac{M_{jt}\lambda|\dot{\phi}_t - \Omega_d|s}{|s| + \delta_1 \exp(-\delta_2 \int \lambda|\dot{\phi}_t - \Omega_d| dt)} - \frac{M_{jt}\lambda|\dot{\phi}_t - \dot{\phi}_b|s}{|s| + \delta_1 \exp(-\delta_2 \int \lambda|\dot{\phi}_t - \dot{\phi}_b| dt)} - \kappa s,
 \end{aligned} \tag{33}$$

where $\delta_1 = 10^{-2}$, $\delta_2 = 10^{-5}$, and $\kappa = 1$ are used in the simulation.

Fig. 9 shows the simulation result using the third switching control (33). It can be observed from the figure that the stick-slip oscillations were suppressed when the controller was switched on at $t = 33$ seconds, and the velocities of the drill bit and the rotary table were stabilized at about $t = 120$ seconds. The sliding-mode controller (30) and (33) is compared with the one proposed in [5] in Fig. 10 for tracking a desired angular velocity $\Omega_d = 3$ rad/sec. As can be seen from the figure, both controllers were switched on at $t = 33$ seconds, and the controller proposed in [5] was unable to suppress the stick-slip oscillations due to parametric uncertainties. Another comparison is made for the two sliding-mode controllers in Fig. 11 for tracking a desired angular velocity $\Omega_d = 4$ rad/sec.

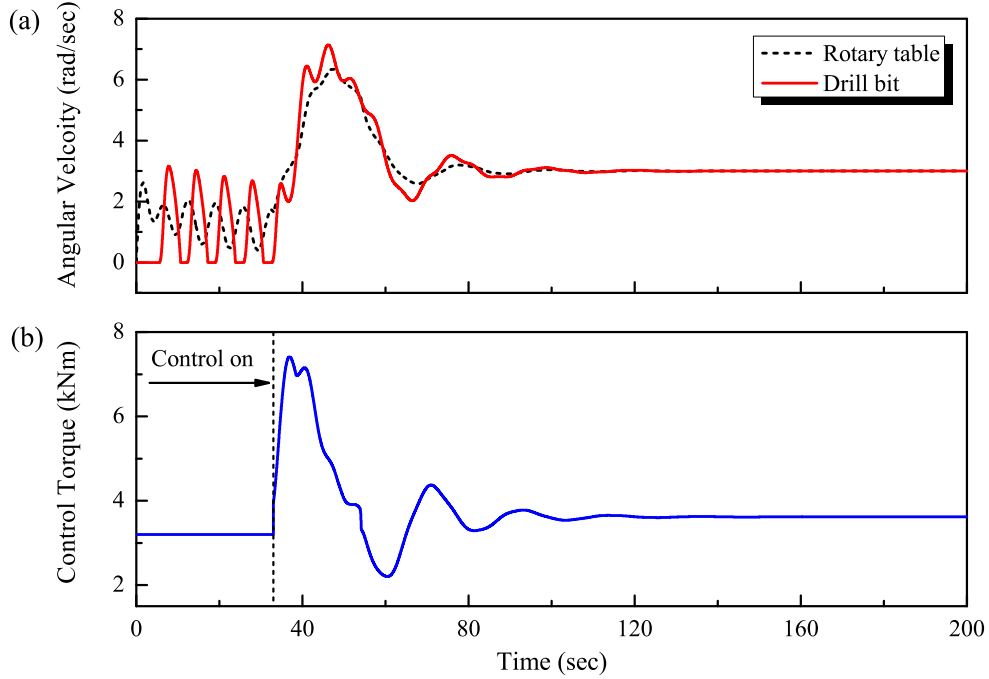


Figure 9: Time histories of (a) angular velocities of the rotary table (black dash line) and the drill bit (red solid line), and (b) the control torque (blue solid line) using the third switching control (33) with $\Omega_d = 3$ rad/sec, $\lambda = 0.3$, $\delta_1 = 10^{-2}$, $\delta_2 = 10^{-5}$, and $\kappa = 1$.

It can be observed that the controller proposed in [5] was able to stabilize the system at about 3 rad/sec, and the drill-string exhibited stick-slip oscillations again when the WOB was increased from 30 kN to 40 kN at $t = 150$ seconds. The reason for such a failure is due to the fact that the controller proposed in [5] does not have a proper switching control gain when the physical parameters of the drill-string are unknown. If the switching control gain is chosen sufficiently large, the chattering will be induced to the system. While for the sliding-mode controller (30) and (33), it has a proper estimation of unknown physical parameters for the switching control gain providing a smooth switching around its sliding surface.

5. Conclusions

Stabilization of multibody drill-strings exhibiting stick-slip oscillations was studied in this paper from the point of view of underactuated system using a lumped-parameter model. The model has one control input acting on the rotary table and multi-degree-

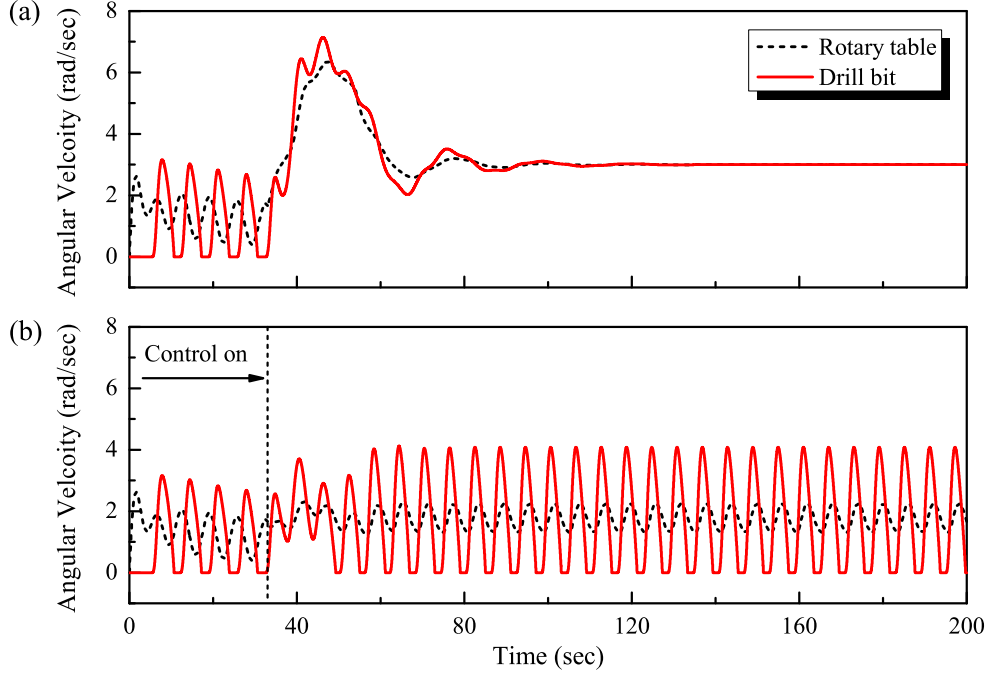


Figure 10: Time histories of (a) angular velocities of the rotary table (black dash line) and the drill bit (red solid line) using the third switching control (33), and (b) angular velocities of the rotary table (black dash line) and the drill bit (red solid line) using the sliding-mode controller in [5] with $\Omega_d = 3$ rad/sec, $\lambda = 0.3$, $\delta_1 = 10^{-2}$, $\delta_2 = 10^{-5}$, and $\kappa = 1$.

of-freedom downhole parts comprising a series of hollow drill pipes, a number of relative thicker drill collars, and a drill bit suffering highly nonlinear friction to be controlled. Three motion regimes for the drill-string model were identified and their equilibria were analyzed accordingly. Sliding-mode control method was applied to the drill-string to suppress stick-slip oscillations whilst tracking a desired rotary speed when its physical parameters were unknown.

Three sliding-mode controllers were studied and their stabilities were proved by using the Lyapunov direct method ensuring that the trajectory of the drill-string can reach and stayed thereafter on the sliding surface in finite time, and the state of the system was able to converge to the desired equilibrium asymptotically. The first proposed sliding-mode controller was based on the traditional discontinuous sign function which caused system chattering. For eliminating the issue, a modified switching controller was proposed by using a continuous function to replace the sign function. Despite the sliding surface does

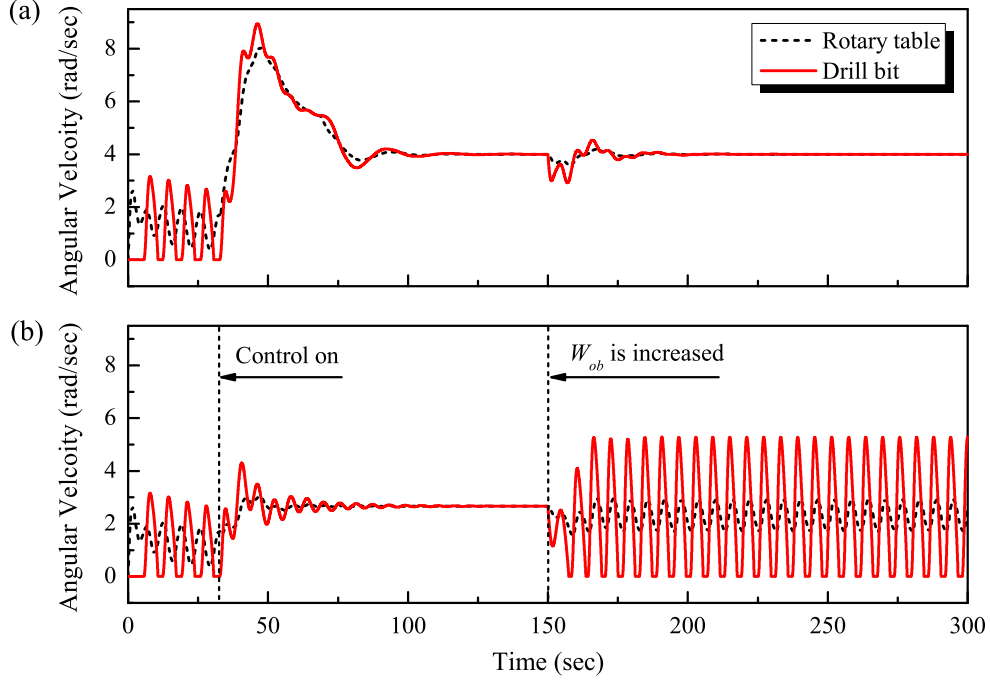


Figure 11: Time histories of (a) angular velocities of the rotary table (black dash line) and the drill bit (red solid line) using the third switching control (33), and (b) angular velocities of the rotary table (black dash line) and the drill bit (red solid line) using the sliding-mode controller in [5] with $\Omega_d = 4$ rad/sec, $\lambda = 0.1$, $\delta_1 = 10^{-2}$, $\delta_2 = 10^{-5}$, and $\kappa = 1$.

not tend to zero any more, it is asymptotically bounded. Hence there is a compromise between a little deterioration of the tracking errors and a large reduction of chattering. In order to overcome this shortcoming, the third switching controller was studied to guarantee that the system was asymptotically stable. A four-degree-of-freedom drill-string model was adopted for simulation studies. Extensive simulation results were given to compare with another existing sliding-mode controller for demonstrating the effectiveness of the proposed controllers and their robustness to parametric uncertainties.

6. Appendix

Proof of Theorem 2. Applying the modified switching control (23), the time derivative of the Lyapunov function (16) becomes

$$\begin{aligned}
\dot{V} &= s[(\hat{c}_p - c_p)(x_1 - x_3) + (\hat{c}_{rt} - c_{rt})x_1 + (\hat{k}_p - k_p)x_2 \\
&\quad + (J_t - \hat{J}_t)\lambda(x_1 - \Omega_d) + (J_t - \hat{J}_t)\lambda(x_1 - x_{2n+5}) \\
&\quad - M_{cp}|x_1 - x_3|\frac{s}{|s|+\delta} - M_{crt}|x_1|\frac{s}{|s|+\delta} - M_{kp}|x_2|\frac{s}{|s|+\delta} \\
&\quad - M_{jt}\lambda|x_1 - \Omega_d|\frac{s}{|s|+\delta} - M_{jt}\lambda|x_1 - x_{2n+5}|\frac{s}{|s|+\delta} - \eta\frac{s}{|s|+\delta} - \kappa s] \\
&\leq |(\hat{c}_p - c_p)(x_1 - x_3)s| + |(\hat{c}_{rt} - c_{rt})x_1s| + |(\hat{k}_p - k_p)x_2s| \\
&\quad + |(J_t - \hat{J}_t)\lambda(x_1 - \Omega_d)s| + |(J_t - \hat{J}_t)\lambda(x_1 - x_{2n+5})s| \\
&\quad - M_{cp}|x_1 - x_3|\frac{s^2}{|s|+\delta} - M_{crt}|x_1|\frac{s^2}{|s|+\delta} - M_{kp}|x_2|\frac{s^2}{|s|+\delta} \\
&\quad - M_{jt}\lambda|x_1 - \Omega_d|\frac{s^2}{|s|+\delta} - M_{jt}\lambda|x_1 - x_{2n+5}|\frac{s^2}{|s|+\delta} - \eta\frac{s^2}{|s|+\delta} - \kappa s^2 \\
&\leq \delta[|(\hat{c}_p - c_p)(x_1 - x_3)| + |(\hat{c}_{rt} - c_{rt})x_1| + |(\hat{k}_p - k_p)x_2| \\
&\quad + |(J_t - \hat{J}_t)\lambda(x_1 - \Omega_d)| + |(J_t - \hat{J}_t)\lambda(x_1 - x_{2n+5})|]\frac{|s|}{|s|+\delta} - \kappa s^2 \\
&\leq \delta[|(\hat{c}_p - c_p)(x_1 - x_3)| + |(\hat{c}_{rt} - c_{rt})x_1| + |(\hat{k}_p - k_p)x_2| \\
&\quad + |(J_t - \hat{J}_t)\lambda(x_1 - \Omega_d)| + |(J_t - \hat{J}_t)\lambda(x_1 - x_{2n+5})|] - \kappa s^2.
\end{aligned}$$

This implies that for the set $\nu = \{s : \|s\| \leq \sqrt{\|\delta\Theta\|/\kappa}\}$, it follows that $\dot{V} < 0, \forall s \in \nu_c$, where ν_c is the complement of ν and Θ is given by

$$\begin{aligned}
\Theta &= |(\hat{c}_p - c_p)(x_1 - x_3)| + |(\hat{c}_{rt} - c_{rt})x_1| + |(\hat{k}_p - k_p)x_2| \\
&\quad + |(J_t - \hat{J}_t)\lambda(x_1 - \Omega_d)| + |(J_t - \hat{J}_t)\lambda(x_1 - x_{2n+5})|.
\end{aligned}$$

This means that the sliding surface does not tend to zero any more, but is bounded as $\|s\| \leq \sqrt{\|\delta\Theta\|/\kappa}$, so that the tracking errors of the system become asymptotically bounded. However there should be a compromise between a little deterioration of the tracking errors and a large reduction of chattering.

7. References

- [1] K. Nandakumar, M. Wiercigroch, Stability analysis of a state dependent delayed, coupled two DOF model of drill-string vibration, *J. Sound and Vibration* 332 (2013) 2575–2592.

- [2] J. F. Breu, The genesis of torsional drillstring vibrations, *SPE Drilling Engineering* (1992) 168–174.
- [3] E. M. Navarro-López, R. Suarez, Practical approach to modelling and controlling stick-slip oscillations in oilwell drillstrings, *Proc of IEEE Int Conf on Control Applications* (2004) 1454–1460.
- [4] E. M. Navarro-López, D. Cortés, Avoiding harmful oscillations in a drillstring through dynamical analysis, *J. Sound and Vibrations* 307 (2007) 152–171.
- [5] E. M. Navarro-López, E. Licéaga-Castro, Non-desired transitions and sliding-mode control of a multi-DOF mechanical system with stick-slip oscillations, *Chaos, Solitons and Fractals* 41 (2009) 2035–2044.
- [6] C. Canudas-de-Wit, F. R. Rubio, M. A. Corchero, D-OSKIL: a new mechanism for controlling stick-slip oscillations in oil well drillstrings, *IEEE. Trans. Control Systems Technology* 16 (2008) 1177–1191.
- [7] H. Puebla, J. Alvarez-Ramirez, Suppression of stick-slip in drillstrings: a control approach based on modeling error compensation, *J. Sound and Vibrations* 310 (2008) 881–901.
- [8] M. Karkoub, M. Zribi, L. Elchaar, L. Lamont, Robust μ -synthesis controllers for suppressing stick-slip induced vibrations in oil well drill strings, *Multibody Syst Dyn* 23 (2010) 191–207.
- [9] E. M. Navarro-López, D. Cortés, Sliding-mode control of a multi-DOF oilwell drillstring with stick-slip oscillations, *Proc of the 2007 American Control Conference* (2007) 3837–3842.
- [10] R. Hernandez-Suarez, H. Puebla, R. Aguilar-Lopez, E. Hernandez-Martinez, An integral high-order sliding mode control approach for stick-slip suppression in oil drillstrings, *Petroleum Science and Technology* 27 (2009) 788–800.

- [11] Y. Liu, H. N. Yu, A survey of underactuated mechanical systems, *IET Control Theory and Applications* 7 (2013) 921–935.
- [12] H. Li, K. Furuta, F. L. Chernousko, A pendulum-driven cart via internal force and static friction, in: *Proceedings of IEEE International Conference on Physics and Control*, St. Petersburg, Russia, 2005, pp. 15–17.
- [13] Y. Liu, H. Yu, T. C. Yang, Analysis and control of a Capsubot, in: *Proceedings of IFAC World Congress*, Seoul, Korea, 2008, pp. 756–761.
- [14] F. Fahimi, Sliding-mode formation control for underactuated surface vessels, *IEEE Trans Robotics* 23 (2007) 617–622.
- [15] R. Yu, Q. Zhu, G. Xia, Z. Liu, Sliding mode tracking control of an underactuated surface vessel, *IET Control Theory and Applications* 6 (2012) 461–466.
- [16] J. Huang, Z. H. Guan, T. Matsuno, T. Fukuda, K. Sekiyama, Sliding-mode velocity control of mobile-wheeled inverted-pendulum systems, *IEEE Transactions on Robotics* 26 (2010) 750–758.
- [17] M. Yue, P. Hu, W. Sun, Path following of a class of non-holonomic mobile robot with underactuated vehicle body, *IET Control Theory and Applications* 4 (2010) 1898–1904.
- [18] Q. H. Ngo, K. S. Hong, Adaptive sliding mode control of container cranes, *IET Control Theory and Applications* 6 (2012) 662–668.
- [19] Q. H. Ngo, K. S. Hong, Sliding-mode antisway control of an offshore container crane, *IEEE/ASME Trans on Mechatronics* 17 (2012) 201–209.
- [20] H. Ashrafiuon, R. S. Erwin, Sliding mode control of underactuated multibody systems and its application to shape change control, *International Journal of Control* 81 (2008) 1849–1858.

- [21] R. Xu, U. Özgüner, Sliding mode control of a class of underactuated systems, *Automatica* 44 (2008) 233–241.
- [22] R. Martinez, J. Alvarez, Y. Orlov, Hybrid sliding-mode-based control of underactuated systems with dry frictions, *IEEE Transaction on Industrial Electronics* 55 (2008) 3998–4003.
- [23] V. Sankaranarayanan, A. D. Mahindrakar, Control of a class of underactuated mechanical systems using sliding modes, *IEEE Transaction on Robotics* 25 (2009) 459–467.
- [24] M. López-Martínez, J. A. Acosta, J. M. Cano, Non-linear sliding mode surfaces for a class of underactuated mechanical systems, *IET Control Theory and Applications* 4 (2010) 2195–2204.
- [25] A. Doris, A. L. Juloski, N. Mihajlovic, W. P. M. H. Heemels, N. V. D. Wouw, H. Nijmeijer, Observer designs for experimental non-smooth and discontinuous systems, *IEEE Trans. Control Systems Technology* 16 (2008) 1323–1332.
- [26] T. Vromen, N. V. D. Wouw, A. Doris, P. Astrid, H. Nijmeijer, Design of an observer-based output-feedback controller to suppress stick-slip oscillations in drill-string systems, in: *Proceedings of the Third International Colloquium on Nonlinear Dynamics and Control of Deep Drilling Systems*, Minneapolis, Minnesota, USA, 2014, pp. 113–119.